8. THE CONTACT DYNAMICS METHOD

8.1 Introduction

The NSCD (Non-Smooth Contact Dynamics) method was presented to the public at the end of the 1980ies by M. Jean and J.J. Moreau (Moreau, 1988; Jean and Moreau, 1992). Its first main field of application was granular mechanics: in comparison to previous discrete element techniques, the NSCD method turned out to be particularly fast and efficient when simulating granular flows, rapid avalanches, segregation, vibration problems of granular materials etc. Since the individual deformations of the grains are usually negligible in these problems, models consisting of perfectly rigid elements were mostly applied at that time. In the first versions the elements were mostly spherical, but later the application of polyhedral elements also became widespread. Contact Dynamics models brought significant scientific achievements in the field of the dynamics of granular materials. While the original papers on NSCD were rather abstract and not very helpful in providing practice-oriented explanations how the method really worked, the paper of Unger and Kertész (2003) brought a leap forward: it gave a clear, detailed introduction to the line of thought of the method, providing valuable help for those who wanted to write their own code and also for those who just wanted to understand the main concept lying behind the software which they were applying in their researches.

For masonry structures and fractured rocks the application of polygonal or polyhedral elements is obviously more suitable than spheres, and the deformability of the elements is often also important to take into consideration. Jean and Moreau (1992) and Jean (1999) introduced the basics of modelling masonry walls with deformable rectangular blocks in NSCD, and Jean developed the software called LMGC that gave realistic results for the quasi-static selfweight problem of planar walls (Jean, 1999). Dubois extended the method, developed the open code LMGC90 (Dubois and Jean, 2006), and offered it to the research community not only for being used by any colleague but also for further developments. LMGC90 can model rigid or deformable, 2D or 3D bodies of spherical or polyhedral shape. Since its release in the early 2000ies several scientists and engineers have applied it for different quasi-static or dynamic problems related to masonry mechanics.

Another available Contact Dynamics software is SOLFEC (Koziara and Bićanić, 2008). SOLFEC aimed at providing a user friendly platform for testing formulations and solution methods. The code implements different (rigid, uniform-strain and finite element) block models, contact detection algorithms, and time integration techniques. SOLFEC is particularly powerful in modelling element deformability with the help of FEM subdivision. In order to have reasonable computation times for real problems, parallelization is also applied in SOLFEC.

The approach of the Contact Dynamics method is very different from other discrete element techniques often applied for masonry analysis, 3DEC (Cundall, 1988) or DDA (Shi, 1992) for instance. In NSCD the basic unit of the analysis is the pair of two randomly chosen elements (contacting or non-contacting). The essence of the method is to find the contact forces transmitted between the two elements of the pair in such a way that during the analyzed time step the two elements should not overlap each other. The contact force is set to zero if the elements would not touch each other without this contact force even at the end of the timestep, and a non-zero force vector is chosen (satisfying conditions corresponding to the

mechanical behavior of the contact) if the two elements have to be slowed down in order to avoid overlap. So the motion of the system is numerically simulated in time through finite time steps, but in such a way that at a considered actual time instant an iterative process sweeps along randomly chosen pairs of the system over and over again, and gradually adjusts the estimated contact forces to get an improving approximation of a state that satisfies the dynamic equations of the system.

Contact recognition and the determination of its geometrical data (i.e. point of action of the contact force, and the normal direction) for polyhedral shapes require more sophisticated techniques than the treatment of spherical elements. The "common plane concept", a very efficient solution of the problem (also applied in 3DEC) is an advantageous and widely applied possibility in NSCD also, and it will be recalled in this section.

Most discrete element methods represent the deformability of the elements either by using an internal FEM mesh in the elements (e.g. 3DEC), or by concentrating the deformations into the contacts, like in the case of the BALL-type models. The calculation of the contact forces between the elements is based on the stiffness characteristics of the contacts in those techniques. The philosophy of NSCD is different. According to the oldest NSCD models, the elements are perfectly rigid, and the contact forces are not related to any stiffness data: the contact forces are calculated to ensure the dynamic equations of the elements, and in addition, they must not violate requirements like the Coulomb limit for friction or the no-tension requirement in cohesionless contacts, but the calculation does not apply any constitutive relations. For statically highly indeterminate systems like e.g. a masonry wall, there exist several alternative force systems that satisfy the equations of motion; NSCD produces randomly one of them, while several equally valid solutions could be received if the problem is calculated repeatedly with the method starting from the same initial state but considering the pairs of elements in different random orders. This non-uniqueness partly explains the doubts why NSCD is not widespread in the analysis of quasi-static engineering problems. On the other hand, since the method is computationally very efficient for the simulation of dynamic problems, NSCD is more popular in earthquake simulations or vibration analysis. It has to be emphasized that there is a general lack of validation studies about the simulation of quasi-static as well as dynamic problems. The attempts of Ceh et al (2015a, 2015b) are very promising in this respect; similar verification examinations (static as well as dynamic) could potentially resolve the existing skepticism of the engineering community and give a fair general evaluation of the strengths and limitations of the technique. So this is a basically important task for future researches.

The aims of Section 8 are (i) to provide an insight into how the method works; (ii) to call the attention on the possible problems and questionable issues the user should be aware of; and (iii) to present a collection of characteristic applications.

This section is built up as follows. The basic variables describing the state of the model are presented in Section 8.2: for the sake of simplicity, in Section 8.2 rigid elements are considered only. Section 8.3 presents the contact model. Section 8.4 introduces the equations of motion and the time integration scheme. Section 8.5 focuses on deformable elements and calls the attention on the most important differences from the rigid-element model. Finally, Section 8.6 introduces different applications of the Contact Dynamics method in the analysis of structural engineering problems.

8.2 The basic variables: Modelling with rigid elements

8.2.1 Geometrical characteristics of the pair of two elements

Unlike in other methods where the basic unit of the analysis is the element or a part of the element around the node, in CD the basic unit is the ***pair of neighbouring elements***. As already mentioned above, the aim of the calculations is to iteratively find the suitable contact forces in all pairs in the system.

For simplicity, the introduction below starts with the case of perfectly spherical three-dimensional elements. A reference point is defined for each element coinciding with its centre of gravity (see Figure 1a).

Focus now on an arbitrarily selected pair of two elements close to (perhaps in contact with) each other. Denote it by *c*. Material points *pc* and *qc* are those having the shortest distance from each other among all material points of the two spheres. Let g^{pq} denote the distance between them. (From now on, *p* is considered as the first and *q* as the second entity in the pair.) If their distance g^{pq} equals to zero, the two material points share the same location and two elements have a (point-like) contact (Figure 1b), where a concentrated contact force can be transmitted between the elements. Unlike in most discrete element techniques, now the contact and the elements do not deform, so contacting elements must move in such a way that there would be no overlap between them: g^{pq} cannot become negative.

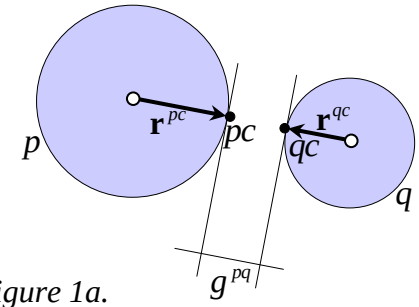

Figure 1a.
The distance g^{pq} between the elements p and q

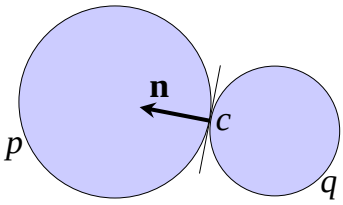

Figure 1b.
The normal vector of the pq contact

Assign an (**n**, **t**, **w**) local coordinate frame to the contact: **n** is the common unit normal of the contact plane (i.e. the common tangent plane), pointing towards element *p* (see Figure 1b); **t** and **w** are an arbitrary pair of orthogonal unit vectors in the contact plane.

For polyhedral elements also a reference point is defined, coinciding again with the centre of gravity (see Figure 2a). In order to decide whether *p* and *q* are in contact at an actual time instant, the two nearest points on the boundary of *p* and *q* are determined (material points *pc* and *qc* respectively). In general case they are node-to-face neighbours, as shown in Figure 2a: in other words, assume for simplicity that the problem to find the two closest points has a unique solution. (The non-unique cases, i.e. edge-to-face neighbours when an edge lies in parallel to a face, or face-to-face neighbours when two planar faces lie parallel to each other, can be modelled as the simultaneous neighbouring pairs of a small finite number of node-to-face pairs. The details will not be considered here.)

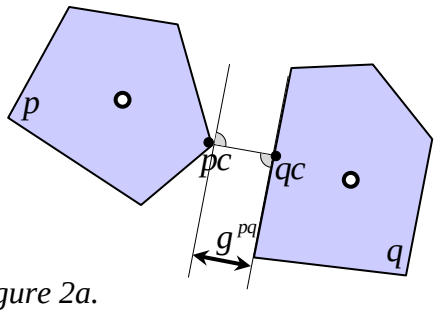

Figure 2a.
Distance g^{pq} between elements p and q

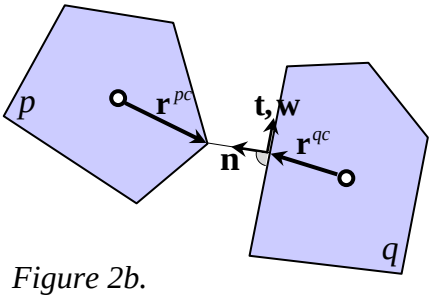

Figure 2b.
The local coordinate system of pair c and the definition of vectors $\mathbf{r}^{pc}$ and $\mathbf{r}^{qc}$

Several possible algorithms are available to find the two closest points. LMGC90 applies the common plane concept (Dubois and Mozul, 2013). To recall it, remember that the common plane can be imagined as a plate that is held loosely between the two polyhedral blocks. If the blocks are brought closer slowly, the plate will be moved by the blocks, and finally will become trapped at some particular position when the blocks come into contact. Whatever the shape and orientation of the blocks (provided they are convex), the plate will take up a position that defines the sliding plane for the two blocks. To carry the analogy a bit further, imagine that the plate is now repelled by the blocks even when they do not touch. As the blocks are brought together, the plate will take up a position midway between them, at a maximum distance from both. The algorithm for locating and moving the common plane can be formulated as an optimization problem: "Maximize the gap between the common plane and the closest vertex". The optimization algorithm applies translations and rotations to the common plane in order to maximize the gap.

The normal vector of the common plane will serve as the contact normal, and the points having the shortest distances from the common plane are the material points *pc* and *qc*. After finding the two closest points, sum up their distances from the common plane, and let g^{pq} denote this sum which is equal to the gap width between the two blocks.

Similarly to the case of spherical elements, assign an (**n**, **t**, **w**) local coordinate frame to the pair in the way shown in Figure 2b. The unit base vector **n** is directed towards the nearest point of *p* (first entity of the pair); base vectors **t** and **w** are an arbitrary pair of orthogonal unit vectors parallel to the contact plane. If the g^{pq} distance equals zero, the two elements form a point-like contact, and a concentrated contact force can be transmitted between the elements. Since the contact and the elements do not deform, the two elements must move in such a way that there would be no overlap between them: the gap width g^{pq} cannot become negative. In addition, the two elements can slide along each other (i.e. the two material points forming the contact point can translate relatively to each other in a direction perpendicular to **n**) only if the frictional limit is reached in the contact.

8.2.2 The reduced contact forces

The force acting on *p* by *q* is $\mathbf{f}^{pc}$, and the force expressed on *q* by *p* is $\mathbf{f}^{qc}$:

$$\mathbf{f}^{pc} = \begin{bmatrix} F_x^{pc}(t) \\ F_y^{pc}(t) \\ F_z^{pc}(t) \end{bmatrix} \quad \text{and} \quad \mathbf{f}^{qc} = \begin{bmatrix} -F_x^{pc}(t) \\ -F_y^{pc}(t) \\ -F_z^{pc}(t) \end{bmatrix},$$

and these can be reduced to the reference points of p and q with the help of the $\mathbf{B}^{pc}(t)$ and $\mathbf{B}^{pc}(t)$ transition matrices, respectively:

$$\mathbf{B}^{pc}(t)=\begin{bmatrix} 1 & 0 & 0 \\ 0 & 1 & 0 \\ 0 & 0 & 1 \\ 0 & -r_z^{pc} & r_y^{pc} \\ r_z^{pc} & 0 & -r_x^{pc} \\ -r_y^{pc} & r_x^{pc} & 0 \end{bmatrix} \quad ; \quad \mathbf{B}^{qc}(t)=\begin{bmatrix} 1 & 0 & 0 \\ 0 & 1 & 0 \\ 0 & 0 & 1 \\ 0 & -r_z^{qc} & r_y^{qc} \\ r_z^{qc} & 0 & -r_x^{qc} \\ -r_y^{qc} & r_x^{qc} & 0 \end{bmatrix} \quad .$$

The vectors $\mathbf{r}^{pc}$ and $\mathbf{r}^{qc}$ point from the reference points to the contact. The reduced forces are then:

$$\mathbf{f}_{red}^{pc}(t)=\mathbf{B}^{pc}(t)\cdot\mathbf{f}^{pc}(t) \quad ; \quad \mathbf{f}_{red}^{qc}(t)=\mathbf{B}^{qc}(t)\cdot\mathbf{f}^{qc}(t) \quad .$$

Summarize these two forces into the 12-scalar ***reduced contact force vector*** of the pair::

$$\mathbf{f}^{pq}(t)=\begin{bmatrix} \mathbf{f}_{red}^{pc}(t) \\ \mathbf{f}_{red}^{qc}(t) \end{bmatrix} \quad .$$

This vector will take part in the equations of motion of the pair.

8.2.3 The relative velocity

The vector $\mathbf{v}^{pq}$ denotes the velocity vector of the (p, q) pair:

$$\mathbf{v}^{pq}(t)=\begin{bmatrix} \mathbf{v}^{p}(t) \\ \mathbf{v}^{q}(t) \end{bmatrix} \quad ,$$

which can be expressed as the time derivatives of the displacements of the reference points (translations and rotations):

$$\mathbf{v}^{p}(t)=\begin{bmatrix} \frac{du_x^p(t)}{dt} \\ \frac{du_y^p(t)}{dt} \\ \frac{du_z^p(t)}{dt} \\ \frac{d\varphi_x^p(t)}{dt} \\ \frac{d\varphi_y^p(t)}{dt} \\ \frac{d\varphi_z^p(t)}{dt} \end{bmatrix} \quad ; \quad \mathbf{v}^{q}(t)=\begin{bmatrix} \frac{du_x^q(t)}{dt} \\ \frac{du_y^q(t)}{dt} \\ \frac{du_z^q(t)}{dt} \\ \frac{d\varphi_x^q(t)}{dt} \\ \frac{d\varphi_y^q(t)}{dt} \\ \frac{d\varphi_z^q(t)}{dt} \end{bmatrix} \quad .$$

Consider now those two material points, *pc* and *qc*, which form the contact. Their velocities, $\mathbf{v}^{pc}$ és $\mathbf{v}^{qc}$, can be expressed again with the help of the $\mathbf{B}^{pc}(t)$ and $\mathbf{B}^{pc}(t)$ transition matrices:

$$\mathbf{v}^{pc}(t) = \mathbf{B}^{pcT}(t) \cdot \mathbf{v}^{p}(t)$$
$$\mathbf{v}^{qc}(t) = \mathbf{B}^{qcT}(t) \cdot \mathbf{v}^{q}(t) \quad .$$

The relative velocity of the contact is the difference of the velocities of the two material points *pc* and *qc*:

$$\boldsymbol{\mu}^{pq}(t) = \begin{bmatrix} \mu_x^{pq}(t) \\ \mu_y^{pq}(t) \\ \mu_z^{pq}(t) \end{bmatrix} := \mathbf{v}^{pc}(t) - \mathbf{v}^{qc}(t)$$

which yields

$$\boldsymbol{\mu}^{pq}(t) = \mathbf{v}^{pc}(t) - \mathbf{v}^{qc}(t) = \left(\mathbf{B}^{pcT}(t) \cdot \mathbf{v}^{p}(t)\right) - \left(\mathbf{B}^{qcT}(t) \cdot \mathbf{v}^{q}(t)\right) \quad .$$

This vector shows the relative translation of point *pc* with respect to point *qc*, so if the two points are already in contact, the n-component of this vector must be positive to exclude overlapping. The tangential component has to be zero if the contact is not sliding, and can be arbitrarily large if the tangential component of the contact force reaches the frictional limit.

8.3 The mechanical conditions of the contacts

In Coulomb-frictional, no-tension contact models the following requirements are to be satisfied in every pair:

(1) If the two elements are in contact, i.e. if $g^{pq} = 0$, then a contact force can be transmitted. If $g^{pq} > 0$, then there is no contact, and no contact force exist in the pair. The case $g^{pq} < 0$ is not possible.
(2) The normal component of the contact force, N^{pq}, can only be negative, i.e. compressional, but otherwise its magnitude ($N^{pq} = \mathbf{f}^{pcT} \cdot (-\mathbf{n})$ or $N^{pq} = \mathbf{f}^{qcT} \cdot \mathbf{n}$) is arbitrary. The (N^{pq}, g^{pq}) relation is shown in Figure 3:

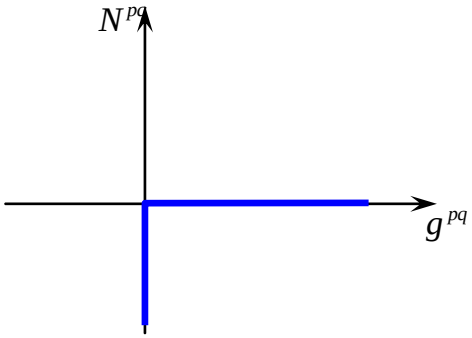

Figure 3.
Normal force versus gap width in CD

(3) The magnitude of the tangential $\mathbf{T}^{pq}$ (which has a *t* and a *w* component) is limited by the Coulomb friction law:

$$\left|\mathbf{T}^{pq}\right| \le -\nu \cdot N^{pq}$$

where ν is the friction coefficient. Figure 4. illustrates this limitation: the vector of the tangential force must point from the origin either to inside the cone (non-sliding contact) or just to the surface of the cone (sliding contact).

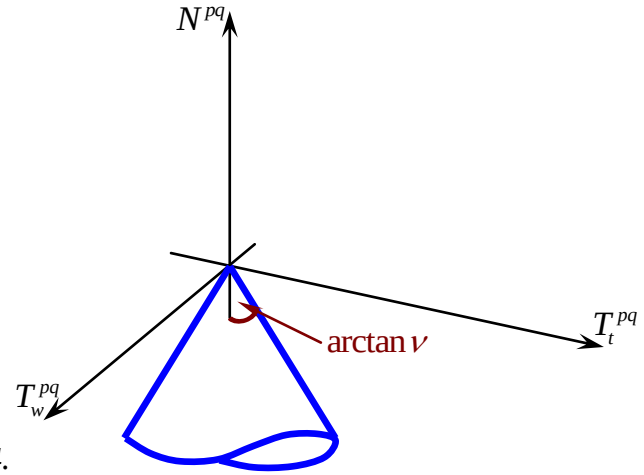

Figure 4.
Columb limit for the tangential force

As long as $\mathbf{T}^{pq}$ is below the friction limit, the tangential component of the relative velocity must be zero (elastic deformation not possible). When reaching the friction limit, the contact starts to slide: the $\boldsymbol{\mu}^{pq}(t)$ relative velocity has to be just opposite to the direction of the $\mathbf{T}^{pq}$ force (the tangential relative translation must not have a component perpendicularly to the frictional force reaching the limit), and the magnitude of $\mathbf{T}^{pq}$ is equal to $-\nu\cdot\mathbf{N}^{pq}$. The magnitude of the relative translation is not limited in the contact model, this can be determined from kinematical considerations.

Without presenting the details, it is interesting to mention that Acary and Jean (2000) introduced more sophisticated representations of the real joint behaviours. They gave suggestions how to model finite tensional or shear resistance, elastic contact behaviour, brittle cohesion or progressive damage behaviour. These extensions of the joint modelling allow the user to give a realistic prediction for structures with mortared contacts. A wide range of such possibilities is available in LMGC90.

8.4 The equations of motion and the iterative solver

Contact Dynamics is a time-stepping method. Its fundamental kinematical unknowns are the time-dependent positions and velocities of the elements. The force-type unknowns are the contact force vectors. They are searched for pair by pair.

Assume that at t_i the state of the system is known: according to the exactness numerically prescribed, the positions and velocities of the elements are given: $\mathbf{u}^p(t_i)\cong\mathbf{u}_i^p$; $\mathbf{v}^p(t_i)\cong\mathbf{v}_i^p$, and the external forces acting on the elements ($\mathbf{f}_i^{p,ext}$) and contact forces for all c ($\mathbf{f}_i^{pc}$) are also known. The external forces are reduced to the reference points; the contact forces act in the point-like contacts. The time-dependence of the external forces is also known (e.g. that the gravitational force is constant), so the external forces are given also in $t_{i+1}=t_i+\Delta t$ ($\mathbf{f}_{i+1}^{p,ext}$). From these data the state of the system at t_{i+1} (contact forces, the positions and the velocities of the elements) is searched for.

CD applies the ***implicit*** version of the Euler method for this search. The basic step for the p and q pair can be written as:

$$\begin{bmatrix} \mathbf{v}_{i+1}^p \\ \mathbf{v}_{i+1}^q \end{bmatrix} := \begin{bmatrix} \mathbf{v}_i^p \\ \mathbf{v}_i^q \end{bmatrix} + \Delta t \cdot \begin{bmatrix} (\mathbf{M}^p)^{-1} & \\ & (\mathbf{M}^q)^{-1} \end{bmatrix} \cdot \begin{bmatrix} \mathbf{f}_{i+1}^p \\ \mathbf{f}_{i+1}^q \end{bmatrix} \quad ;$$

$$\begin{bmatrix} \mathbf{u}_{i+1}^p \\ \mathbf{u}_{i+1}^q \end{bmatrix} := \begin{bmatrix} \mathbf{u}_i^p \\ \mathbf{u}_i^q \end{bmatrix} + \Delta t \cdot \begin{bmatrix} \mathbf{v}_{i+1}^p \\ \mathbf{v}_{i+1}^q \end{bmatrix} \quad .$$

Here $\mathbf{f}_{i+1}^p$ and $\mathbf{f}_{i+1}^q$ denote the resultants of the external and all contact forces acting on p and q respectively, being reduced to the reference points. (Note that according to the implicit scheme, the velocities and accelerations belonging to the end of the time interval are considered to be valid along the whole interval.) These reduced forces are

$$\begin{bmatrix} \mathbf{f}_{i+1}^p \\ \mathbf{f}_{i+1}^q \end{bmatrix} := \begin{bmatrix} \mathbf{f}_{i+1}^{p,ext} + \sum_{(pk)} \mathbf{B}^{pk} \cdot \mathbf{f}_{i+1}^{pk} \\ \mathbf{f}_{i+1}^{q,ext} + \sum_{(qk)} \mathbf{B}^{qk} \cdot \mathbf{f}_{i+1}^{qk} \end{bmatrix} \quad .$$

Summation over index pk runs along all contacts of element p , including the just analysed contact c as well. Similarly, index qk runs along all contacts of q.

The transition matrices are assumed to be constant during the (t_i, t_{i+1}) time interval, and equal to their values at t_i. Indeed, if the displacement increments are small during the timestep, the modification of the vectors pointing from the reference points to the contacts is negligible.

Collect the mass and rotational inertia of the elements into the matrices $\mathbf{M}^p$ and $\mathbf{M}^q$, which have the following form in the case of spherical elements:

$$\mathbf{M}^p = \begin{bmatrix} m^p & & & & & & \\ & m^p & & & & & \\ & & m^p & & & & \\ & & & I^p & & & \\ & & & & I^p & & \\ & & & & & I^p & \end{bmatrix} \quad .$$

(Note that because of the spherical symmetry, these matrices are constant in time.) For non-spherical elements the inertia matrices have the following form:

$$\mathbf{M}^p = \begin{bmatrix} m^p & & & & & \\ & m^p & & & & \\ & & m^p & & & \\ & & & I_{xx}^p & I_{xy}^p & I_{xz}^p \\ & & & I_{yx}^p & I_{yy}^p & I_{yz}^p \\ & & & I_{zx}^p & I_{zy}^p & I_{zz}^p \end{bmatrix}$$

The lower right block depends on the actual orientation of the element so it varies with time.

In order to determine the velocity of the pair ($\mathbf{v}_{i+1}^{pq}$), the resultants $\mathbf{f}_{i+1}^{p}$ and $\mathbf{f}_{i+1}^{q}$ should be known. So, in addition to the external forces acting at t_{i+1}, the contact forces should also be known at the end of the timestep. The Contact Dynamics models search for these contact forces with the help of an ***iterative solver*** (which has to be performed over and over again at every timestep, as the contact forces change with time).

The solver sweeps along all pairs of neighbouring or nearly contacting elements. When considering a given pair, an approximation is given based on the equations of motion of the pair (see the details below), so that the conditions assumed on the mechanical behaviour would be satisfied: no overlap; Coulomb-friction etc. Then a next pair is considered. After all pairs were swept over, the solver starts the pairs from the beginning, and it is repeated over and over again, until the next approximations are already sufficiently close to the previous ones. It means that the contact forces belonging to t_{i+1} have been found, and the next time step can follow.

The length of the timestep can be relatively large in comparison to models using explicit time integration (e.g. PFC or 3DEC). As explained by Radjai and Richefeu (2009), the limit on the timestep length is given by the occurrence of cumulative numerical errors leading to undesired excess overlaps between the particles. They suggest that a typical value for time step length is 10^{-4} sec for a system that consists of 10^4 rigid elements.

The approximation of the contact force in the pair (p, q) is based on the equations of motion of that pair. Before turning onto the details, a few notations have to be introduced:

For element p, reduce to the reference point all those forces (external and contact forces) acting at t_{i+1}, ***except from*** the force expressed by element q through contact c:

$$\mathbf{f}_{red,i+1}^{p,no\_c} := \mathbf{f}_{i+1}^{p,ext} + \sum_{pk \neq pc} \mathbf{f}_{red,i+1}^{pk} \quad .$$

The $\mathbf{f}_{i+1}^{pk}$ contact force is only an actual approximation of the force indeed acting in contact pk at t_{i+1}; it receives new and new values during the iterations. (At the beginning of the analysis of the time step the contact forces are approximated to be the same as their final, just determined values at the end of the previous time step, which is the same as the beginning of the just analysed timestep.)

Similarly, reduce all the forces acting at t_{i+1} on q – except from that force acting in qc – to the reference point of q:

$$\mathbf{f}_{red,i+1}^{q,no\_c} := \mathbf{f}_{i+1}^{q,ext} + \sum_{qk \neq qc} \mathbf{f}_{red,i+1}^{qk} \quad ,$$

and collect the two vectors into a hypervector:

$$\mathbf{f}_{red,i+1}^{pq,no\_c} := \begin{bmatrix} \mathbf{f}_{red,i+1}^{p,no\_c} \\ \mathbf{f}_{red,i+1}^{q,no\_c} \end{bmatrix} \quad .$$

Summarize the two transition matrices belonging to c into a hypermatrix:

$$\mathbf{B}^{pq} := \begin{bmatrix} \mathbf{B}^{pc} \\ -\mathbf{B}^{qc} \end{bmatrix}$$

and the matrices of inertia of p and q into a block-diagonal matrix, whose inverse is:

$$\left(\mathbf{M}^{pq}\right)^{-1} := \begin{bmatrix} \left(\mathbf{M}^{p}\right)^{-1} & \mathbf{0} \\ \mathbf{0} & \left(\mathbf{M}^{q}\right)^{-1} \end{bmatrix} .$$

Later the following two matrices will also be necessary:

$$\left(\mathbf{M}^{pq}\right)^{-1} := \mathbf{B}^{pqT}\left(\mathbf{M}^{pq}\right)^{-1}\mathbf{B}^{pq} ,$$

and

$$\mathbf{M}^{pq} := \left(\mathbf{B}^{pqT}\left(\mathbf{M}^{pq}\right)^{-1}\mathbf{B}^{pq}\right)^{-1} .$$

And now the equations of motion of the pair (*p*, *q*) can be compiled. First, the equations belonging to the end of the time interval can separately be written as:

$$\frac{1}{\Delta t}\begin{bmatrix} \mathbf{v}_{i+1}^{p} - \mathbf{v}_{i}^{p} \\ \mathbf{v}_{i+1}^{q} - \mathbf{v}_{i}^{q} \end{bmatrix} = \left(\mathbf{M}^{pq}\right)^{-1} \cdot \begin{bmatrix} \mathbf{f}_{red,i+1}^{p,no\_c} + \mathbf{f}_{red,i+1}^{pc} \\ \mathbf{f}_{red,i+1}^{q,no\_c} + \mathbf{f}_{red,i+1}^{qc} \end{bmatrix} .$$

Multiply both sides by $\mathbf{B}^{pqT}$ from the left:

$$\frac{1}{\Delta t}\left[\boldsymbol{\mu}_{i+1}^{pq} - \boldsymbol{\mu}_{i}^{pq}\right] = \mathbf{B}^{pqT}\left(\mathbf{M}^{pq}\right)^{-1} \cdot \mathbf{f}_{red,i+1}^{pq,no\_c} + \\ + \mathbf{B}^{pqT}\left(\mathbf{M}^{pq}\right)^{-1}\mathbf{B}^{pq} \cdot \mathbf{f}_{i+1}^{pc}$$

(it was taken into consideration that $\mathbf{f}_{i+1}^{qc} = -\mathbf{f}_{i+1}^{pc}$). After some rearrangements:

$$\boldsymbol{\mu}_{i+1}^{pq} - \left(\boldsymbol{\mu}_{i}^{pq} + \Delta t \cdot \mathbf{B}^{pqT}\left(\mathbf{M}^{pq}\right)^{-1} \cdot \mathbf{f}_{red,i+1}^{pq,no\_c}\right) = \Delta t \cdot \left(\mathbf{M}^{pq}\right)^{-1}\mathbf{f}_{i+1}^{pc} .$$

It is easy to notice that on the left side the vector in the parentheses means that relative velocity which would occur in the contact at t_{i+1} if $\mathbf{f}_{i+1}^{pc}$ is zero, i.e. if there is no force in the contact. This vector will have a special importance in the forthcoming derivation, so a special notation is given to it:

$$\boldsymbol{\mu}_{i+1}^{pq,no\_c} := \left(\boldsymbol{\mu}_{i}^{pq} + \Delta t \cdot \mathbf{B}^{pqT}\left(\mathbf{M}^{pq}\right)^{-1} \cdot \mathbf{f}_{red,i+1}^{pq,no\_c}\right) .$$

The equations of motion can now be written as:

$$\boldsymbol{\mu}_{i+1}^{pq} = \boldsymbol{\mu}_{i+1}^{pq,no\_c} + \Delta t \cdot \left(\mathbf{M}^{pq}\right)^{-1}\mathbf{f}_{i+1}^{pc}$$

where $\boldsymbol{\mu}_{i+1}^{pq}$ and $\mathbf{f}_{i+1}^{pc}$ are the unknowns. So the equations of motion give the relation between the unknown contact force and the unknown relative velocity belonging to the contact. This will be the starting point of the forthcoming calculations.

Finally the normal and tangential components of the relative velocity vector of the contact will be needed:

$$\mu_{n}^{pq} = \mathbf{n}^{T} \cdot \boldsymbol{\mu}^{pq} ; \quad \boldsymbol{\mu}_{tw}^{pq} = \boldsymbol{\mu}^{pq} - \mu_{n}^{pq} \cdot \mathbf{n}$$

(Remember that $\boldsymbol{\mu}^{pq}$ denoted the velocity of the material point *pc* relative to the material point *qc*. Hence a positive μ_{n}^{pq} means increasing gap between the two material points.) Since the vector $\boldsymbol{\mu}_{i+1}^{pq,no\_c}$ belonging to the time instant t_{i+1} can directly be calculated from the already

existing approximations of all other contact forces except from *c*, the components $\mu_{n,i+1}^{pq,no\_c}$ and $\boldsymbol{\mu}_{tw,i+1}^{pq,no\_c}$ can also be determined, while the components of the vector $\boldsymbol{\mu}_{i+1}^{pq}$ are unknowns.

The unknown $\boldsymbol{\mu}_{i+1}^{pq}$ and $\mathbf{f}_{i+1}^{pc}$ vectors are determined in three steps:

Step 1. First decide whether the two elements will be in contact at t_{i+1} : calculate how large will the gap be between them, assuming zero contact force:

$$g_{i+1}^{pq,no\_c} = g_i^{pq} + \mu_{n,i+1}^{pq,no\_c} \cdot \Delta t \quad .$$

A positive result means that there will be no contact at t_{i+1} , and the analysis of another pair can immediately follow. A negative result, on the other hand, means that without a contact force the elements *p* and *q* would overlap, so an $\mathbf{f}^{pc}$ contact force is needed to avoid the overlap. In this case Step 2. follows.

Step 2. The contact force should modify the velocities of the two elements in such a way that instead of overlapping, they would exactly touch each other at the end of the time step. In Step 2. the aim is to determine $\mathbf{f}_{i+1}^{pc}$ that satisfies the following two conditions:

(i) at t_{i+1} the gapwidth between *p* and *q* is exactly zero:

$$g_i^{pq} + \mu_{n,i+1}^{pq} \cdot \Delta t = 0$$

(ii) the contact does not slide, so the tangential component of the relative translation is zero:

$$\left|\boldsymbol{\mu}_{tw,i+1}^{pq}\right| = 0$$

To satisfy these two conditions, the relative velocity of the contact should be:

$$\boldsymbol{\mu}_{i+1}^{pq} = -\frac{1}{\Delta t} g_i^{pq} \cdot \mathbf{n}$$

(the negative sign means that if the gapwidth was larger than zero, then *p* should get closer to *q* to touch it).

The $\mathbf{f}_{i+1}^{pc}$ has to be such a force that if continuously acting between *p* and *q* during (t_i, t_{i+1}), at t_{i+1} the relative velocity would be just equal to $\boldsymbol{\mu}_{i+1}^{pq}$. From the equations of motion, this force turns out to be equal to:

$$\mathbf{f}_{i+1}^{pc} = \frac{1}{\Delta t}\mathbf{M}^{pq} \cdot \left(-\frac{1}{\Delta t} g_i^{pq}\mathbf{n} - \boldsymbol{\mu}_{i+1}^{pq,no\_c} \right) .$$

Now the question is whether this force violates the constitutive conditions. There were two conditions on the components of the contact forces. The first one required the normal force a compression. This is automatically satisfied because of Step 1. The second one was the Coulomb-condition:

$$\left|\mathbf{T}_{i+1}^{pc}\right| \le -\boldsymbol{\nu} \cdot N_{i+1}^{pc}$$

If this holds for the calculated $\mathbf{f}_{i+1}^{pc}$, then the analysis of the (*p*, *q*) pair is ready, and a next pair can follow. However, if the tangential component exceeds the friction limit, then the calculated contact force cannot be transmitted in the contact: the contact slides, which means that the tangential component of $\boldsymbol{\mu}_{i+1}^{pq}$ is not zero, and the calculation based on zero tangential component should be corrected. This correction is done in Step 3.

Step 3. In a sliding contact the tangential force component has to satisfy the following to conditions, and – as the third condition – the equations of motion:

(i) The contact is sliding, so the magnitude of the tangential force component is equal to the Coulomb-limit:

$$\left|\mathbf{T}_{i+1}^{pc}\right| = -\nu \cdot N_{i+1}^{pc}$$

(ii) The direction of the tangential relative velocity is just opposite to the direction of the tangential force component:

$$\frac{\mathbf{T}_{i+1}^{pc}}{\left|\mathbf{T}_{i+1}^{pc}\right|} = -\frac{\boldsymbol{\mu}_{tw,i+1}^{pq}}{\left|\boldsymbol{\mu}_{tw,i+1}^{pq}\right|}$$

(iii) the equations of motion:

$$\mathbf{f}_{i+1}^{pc} = -\frac{1}{\Delta t}\mathbf{M}^{pq} \cdot \left(\frac{1}{\Delta t} g_i^{pq} \mathbf{n} + \boldsymbol{\mu}_{i+1}^{pq,no\_c} - \boldsymbol{\mu}_{tw,i+1}^{pq} \right)$$

From these conditions the unknowns $\mathbf{f}_{i+1}^{pc}$ és $\boldsymbol{\mu}_{i+1}^{pq}$ can be calculated, and the analysis of the (*p*, *q*) pair is ready. The next pair can follow.

These calculations introduced above give an approximation for the contact force in a pair, assuming that all other contact forces are unchanged and keep their values last approximated. When turning to the next pair, the latest approximations in other pairs are applied. Proceeding from pair to pair this way, an approximation is received for the whole system of contact forces. By sweeping through the complete set of contacts and nearly-contacting pairs over and over again, the results (at least, hopefully) get closer and closer to what should really exist at t_{i+1}. (Note that convergence is still an open issue: a precise proof does not exist in the literature.) The modifications caused by the consecutive iteration cycles cause smaller and smaller modifications in the contact forces; and the iteration can be terminated as the modifications decrease under a prescribed threshold. Now the state belonging to t_{i+1} has been found, and a new time step can be analysed.

The order according to which the pairs are considered within an iteration step is ***random***; the only requirement is that every pair should be considered once. In the next iteration steps the ordering is different, prescribed also by a random number generator.

If the same problem is analysed twice, by starting the random number generator from two different initiations, the two resulting contact force systems will be different. This non-uniqueness of the solution has been emphasized by e.g. Jean (1999) or Moreau (2006). Indeed, for a statically highly indeterminate system several equilibrated force systems can be found, and without the flexibility data the "correct" one cannot be selected. In addition, the possibility of frictional sliding makes the solution history dependent. Moreau (2006) gave a very interesting discussion on the non-uniqueness of the solution. However, experiences on granular assemblies, e.g. Radjai and Richefeu (2009), show that though the order of the pairs greatly affect the individual contact forces and even the topology of the system, the overall, "macro" characteristics like average stress tensor or frequency diagram of contact force magnitudes remain the same, apart from slight statistical deviations. This conclusion might be valid for masonry systems too, but the existing investigations up to the present are still insufficient to draw reliable conclusions.

8.5 Modelling with deformable elements

8.5.1 Elements and contacts

Blocks in NSCD can be made deformable either by applying a uniform strain field in the whole block (like in DDA), or by using a finite element subdivision inside the blocks. Koziara and Bicanic (2008) presented the possibility to apply uniform-strain blocks. They used the term "pseudo-rigid bodies" to the approach, and suggested it as an intermediate model between perfectly rigid blocks and FEM-divided bodies. A finite element subdivision seems to be more appropriate for practical problems particularly in the case of complex block shapes or significantly varying stress fields inside the blocks.

Jean (1999) applied uniform-strain finite element subdivision as the simplest possibility for FEM meshing. A two-dimensional illustration is shown in Figure 5: a rectangular block is subdivided into eight uniform-strain triangular elements.

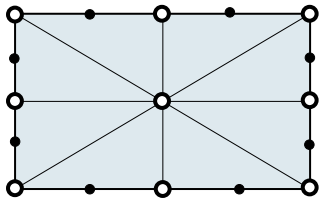

Figure 5.
Deformable 2D block consisting of triangular finite elements:
O: nodes; • : potential contact points

The mass of the element is distributed to the nodes (denoted by empty dots in Figure 5). The degrees of freedom are the translations of these nodes, which means that nodal rotations are not considered in the model: the usual strain field of classical continua is the basis of stress calculations (no Cosserat- or other non-classical continua are applied).

The equations of motion of a node specify the relations between the translational accelerations of the node, and between the forces reduced to the node:

→ mass-proportional forces (e.g. selfweight);
→ external loads (including velocity-proportional forces like drag force);
→ contact forces acting on any face belonging to the analysed node;
→ internal forces: effect of stresses inside elements belonging to the analysed node.

The determination of the point where the contact forces act on the considered element is a crucial issue. Instead of performing a detailed analysis of the force distribution along the contact surfaces, a simplified approach is used. Dark dots in Figure 5 denote the candidates for contact points with neighbouring faces. They are chosen to be in the centre of the finite element face. Their actual position can be linearly interpolated from the nodes forming the face where the candidate contact point is located. If such a candidate touches a neighbouring face, contact forces act on the element at this contact point. The contact forces are then reduced to the nodes, according to the usual way at uniform-strain finite elements.

Note that LMGC90 offers more sophisticated FEM meshing options too (Dubois and Mozul, 2013), and in those cases the interpolation of contact point position and the reduction of the contact force become more complicated.

8.5.2 The non-uniqueness of the solution

Similarly to the rigid-element case, the equations of motion of the whole system of deformable blocks at a time instant *t* can be written in the following general form:

$$\mathbf{M}\mathbf{a}(t)+\mathbf{C}\mathbf{v}(t)+\mathbf{K}(t)\Delta\mathbf{u}(t)=\mathbf{f}(t)\,.$$

In this expression the meaning of the terms are as follows:

→ $\Delta\mathbf{u}(t)$ is the hypervector containing the nodal translations from an initial deformation-free configuration to the actual nodal positions at *t*;

→ $\mathbf{v}(t)$ and $\mathbf{a}(t)$ are its first and second time derivatives (hypervectors of nodal velocities and nodal accelerations respectively);

→ $\mathbf{K}(t)$ is the stiffness matrix expressing the elastic properties of the finite elements: its *j*-th column contains the opposite of nodal forces which arise when a unit translation is introduced at the *j*-th scalar of $\Delta\mathbf{u}(t)$;

→ $\mathbf{C}(t)$ is the damping matrix: its j-th column contains the opposite nodal forces if a unit velocity occurs at the *j*-th scalar of $\mathbf{v}(t)$;

→ $\mathbf{M}(t)$ is the block diagonal mass matrix that consists of as many blocks as the number of nodes, every block in it is a diagonal matrix containing three elements each of which being equal to the mass assigned to the corresponding node;

→ $\mathbf{f}(t)$ is the hypervector of the external loads and contact forces reduced to the nodes.

Assuming that: (i) the structure is statically indeterminate or, at least, determinate, (ii) sliding, cracking or other abrupt changes of material behaviour can be excluded during $\Delta\mathbf{u}$, (iii) $\Delta\mathbf{u}$ is so small that $\mathbf{K}$ remains approximately the same as in the initial configuration, and (iv) loads are quasi-static, then since the stiffness matrix is invertible and constant, the iterative solver introduced in Section 2.4 corresponds to a Gauss-Seidel relaxation solution of the equilibrium position corresponding to the given loads. In this case the solution would be unique. If the structure is kinematically indeterminate but nonlinearities do not occur, then $\mathbf{K}$ is singular (though constant), and for general quasi-static loads the iterative solver does not lead to an equilibrium state but to an accelerating motion of the elements. (This phenomenon can characterize only an initial, small-displacement range of the behaviour.) Large displacements led to the gradual modification of $\mathbf{K}$. When sliding, contact cracking, or other dissipative material nonlinearities occur, $\mathbf{K}$ varies, and the solution becomes history-dependent and non-unique. In this case (similarly to the rigid-element case) repeated solutions of the same problem may differ from each other. Even if the system converges to an equilibrium, there are various paths of motions possible, and they typically lead to different equilibrium states. The user should be aware of this feature of Contact Dynamics. Acary and Jean (2000) discuss the problem and suggest a few possibilities to deal with the issue.

8.6 Applications

The Contact Dynamics Method has been rather popular among physicists studying granular dynamics problems (e.g. Daudon et al, 1997; Radjai et al, 1998; Unger et al, 2004). In the field of masonry mechanics most applications are related to seismic simulations, though a few examples on quasi-static analysis can also be found in the literature as shown by the applications below.

Chetouane et al (2005) applied the Contact Dynamics method for the simulation of Pont Julien, a 1st-century BC roman bridge in South France, in Vaucluse. They built a 2D model with dry frictional contacts, and compared the results provided by the rigid-element

and the deformable-element modelling approaches for quasi-static case. The load was the selfweight of the structure. Principal stress directions, hydrostatic stress components and contact states were compared. They found that while the computation time was definitely longer, deformable elements provided more realistic results. The 3D analysis of the same bridge under the effect of flood was published in Rafiee and Vinches (2013). The selfweight of those parts of the structure being under water level was decreased according to buoyancy, and increasing crosswise horizontal forces acting on the pillars at different levels were tested. A variety of failure mechanisms were revealed.

Raifee et al (2008a) modelled the Roman aqueduct in Arles, near Fontvielle, France. The aqueduct was collapsed, but the reasons of the failure were unknown. 3D rigid elements with dry frictional contacts were applied in the NSCD model of the aqueduct. Starting from an assumed undamaged initial geometry of the structure, selfweight and then sinusoidal seismic excitations were applied. The dynamic effects produced a cracked state of the structure, whose similarities to the in situ state suggested that a seismic event could be the reason of the destruction of the structure around 150 AD.

Rafiee et al (2008b) prepared 2D and 3D models of the amphitheatre in Nimes, one of the most beautiful and best preserved Roman arenas. The elements were rigid and deformable in their 2D models, and rigid in the 3D model, with dry contacts in all cases. In addition to selfweight, an artificial seismic vibration was simulated. The most vulnerable parts of the structure could be identified this way, so that a future restoration can take this knowledge into consideration. The amphitheatre was analysed a few years later by Bagnéris et al (2013), also with LMGC90. Rigid 3D elements were applied to model a similar part of the arena as in Rafiee et al (2008b). In Bagnéris et al (2013) the results provided by the rigid-element model were then applied to an individual block at the bottom of a pillar, and the behaviour of this block was simulated by using deformable elements in a linearly elastic FEM model. The pressure acting on this block along its boundaries was made non-uniform in the FEM analysis, in different ways (a peripheral support and surface roughness was produced by randomly translating the position of the FEM nodes perpendicularly to the surface). The results show that at some locations the magnitude of principle stresses could increase with 1 or even 2 orders of magnitude because of the contact surfaces being not perfectly planar. This phenomenon may lead to local damages that may modify the distribution of the internal forces in the structure provided by the NSCD calculation. (The authors also considered the effect f water infiltration, but that analysis is already out of the scope of an introduction to the NSCD method.)

Isfeld and Shrive (2015) modelled the cross-section of the wall of Prince of Wales Fort (built in the early 18^{th} century) in Canada. The external part of the wall is made of cut stones lying on each other on approximately planar faces, while the core of the wall consists of ribble-like uncut stone pieces. The old mortar between the stone blocks degraded, weakened and was washed out during the centuries. In the model the external stones were represented by rigid polygons and the core consisted of rigid circular elements. The contacts were cohesive: the normal and shear strength were set to several different values in the different tests, and for every case the walls were tried to be equilibrated under selfweight. It was decided this way whether for the different joint material parameters the walls were stable or unstable. (The typical failure modes were also determined.) The authors concluded that stability could be improved by injecting grout into the walls.

Lancioni et al (2013) analysed a medieval Italian church, Santa Maria in Portuno. After its enlargement in the 11th century, the building had a nave and two aisles. For today only the nave remained, and one of the aims of the numerical analysis was to verify whether the collapse of the aisles could be caused by a 13th-century earthquake in the region. The authors applied rigid 3D polyhedral elements with dry frictional contacts. The geometry of the structure was reconstructed from the ruins that were found on the site. The model consisted of four macro-elements, corresponding to the following four main components of the structure: (1) the façade, (2) a longitudinal wall of the nave, (3) and external wall, and (4) the three apses. The 2009 L'Aquila earthquake was simulated. The analysis pointed out the most dangerous collapse mechanisms, and conclusions could be drawn regarding the expedient reinforcement of the structure.

Though the above examples demonstrate that the Contact Dynamics technique is able to simulate practical problems in an apparently realistic way, most of the applications up to now are poor in (or completely lack) a quantitative validation of the applied numerical model. An industry-inspired attempt to improve this situation can be found in the recent publications Ceh et al (2015a, 2015b). The authors conducted laboratory experiments and SOLFEC simulations on the same problem: multiple-block stacks subjected to base accelerations were analysed in both ways. Well-documented experimental and numerical tests like this would be very valuable for engineers who plan to apply a Contact Dynamics software for practical problems. With more validation studies, and with sufficiently increasing hardware capacities in the forthcoming years, the Contact Dynamics method may become a powerful tool in the everyday engineering practice.

Questions

8.1. Write the equations of motion of a pair in CD, and explain the meaning of the quantities in it! How to reduce the contact force vector to the reference points of the two elements? How to express the relative velocity of the contact in terms of the velocity vectors of the two elements?
8.2. Describe the mechanics of the contacts in CD!
8.3. Explain the analysis of a time step in CD! How the "iterative solver" works?
8.4. Explain the main idea of using deformable elements in CD!
8.5. Why is the solution given by CD non-unique?